Finite element modelling of heat transfer in ground source energy systems with heat exchanger pipes

Klementyna A. Gawecka

Teaching Fellow, Dept. of Civil & Environmental Engineering, Imperial College London, London SW7 2AZ, U.K. E-mail: klementyna.gawecka09@imperial.ac.uk

David M. G. Taborda

Senior Lecturer, Dept. of Civil and Environmental Engineering, Imperial College London, London SW7 2AZ, U.K. E-mail: d.taborda@imperial.ac.uk

David M. Potts

GCG Professor of Geotechnical Engineering, Dept. of Civil & Environmental Engineering, Imperial College London, London SW7 2AZ, U.K. E-mail: d.potts@imperial.ac.uk

Eleonora Sailer

Ph.D. Candidate, Dept. of Civil & Environmental Engineering, Imperial College London, London SW7 2AZ, U.K. E-mail: eleonora.sailer13@imperial.ac.uk

Wenjie Cui

Research Associate, Dept. of Civil and Environmental Engineering, Imperial College London, London SW7 2AZ, U.K. (Corresponding Author: w.cui11@imperial.ac.uk)

Lidija Zdravković

Professor of Computational Geomechanics, Dept. of Civil & Environmental Engineering, Imperial College London, London SW7 2AZ, U.K. E-mail: l.zdravkovic@imperial.ac.uk

Abstract

Ground source energy systems (GSES) utilise low enthalpy geothermal energy and have been recognised as an efficient means of providing low carbon space heating and cooling. This study focuses on GSES where the exchange of heat between the ground and the building is achieved by circulating a fluid through heat exchanger pipes. Although numerical analysis is a powerful tool for exploring the performance of such systems, simulating the highly advective flows inside the heat exchanger pipes can be problematic. This paper presents an efficient approach for modelling these systems using the finite element method (FEM). The pipes are discretised with line elements and the conductive-advective heat flux along them is solved using the Petrov-Galerkin FEM instead of the conventional Galerkin FEM. Following extensive numerical studies, a modelling approach for simulating heat exchanger pipes, which employs line elements and a special material with enhanced thermal properties, is developed. The modelling approach is then adopted in three-dimensional simulations of two thermal response tests, with an excellent match between the computed and measured temperatures being obtained.

Keywords: heat transfer; ground source energy system; heat exchanger pipe; finite element modelling; thermal response test

Introduction

Fossil fuel reserves are diminishing and global energy consumption is increasing due to a constantly expanding population enjoying improved living standards, meaning that there is a growing concern over the management of the Earth's resources. Rising energy prices, as well as government sustainability policies encourage the use of renewable energy sources. This paper focuses on one type of renewable energy: low enthalpy geothermal energy which is concerned with temperatures of less than 40 °C and usually depths of up to 300 m below the ground surface (Banks, 2012). Ground source energy systems (GSES) are installations which utilise this thermal energy and have been recognised as a reliable and efficient means of providing space heating and cooling. In some of these systems, the exchange of energy with the ground is achieved by circulating a fluid around loops of so-called heat exchanger pipes buried (either horizontally or vertically) in the ground.

The heat transfer mechanism taking place in heat exchanger pipes can be described in terms of two components – axial and radial. Along the length of the pipes (i.e. in the axial direction), the energy is transported by forced convection which includes both conduction (i.e. a heat transfer process associated with movement of molecules) and advection (i.e. transfer of heat by bulk motion of the fluid). Clearly, due to the high fluid velocities, the latter is dominant. The heat transfer in the radial direction is illustrated in terms of temperature changes in Figure 1 and consists of heat conduction through the pipe wall (ΔT_{wall}) and convective heat transfer in the film layer (i.e. a layer of fluid adjacent to the pipe wall where flow regime changes from turbulent in the centre of the pipe to laminar at its surface creating a resistance to heat flow) on the inside of the pipe wall (ΔT_{int}). The convective heat transfer on the outside of the pipe wall (ΔT_{ext}) may be due to the resistance caused by the film layer if the pipe is surrounded by a fluid, or due to contact resistance arising from an imperfect contact between the pipe and a solid material. In all cases, the convective heat flux, Q_c, on the inside and the outside of the pipe wall is described by the Newton's law of cooling as:

$$Q_{c,i} = h_i \Delta T_i \qquad (1)$$

where h is the convective heat transfer coefficient, ΔT is the temperature difference betweent the fluid (or the external solid) and the pipe surface, and the subscript i indicates either internal convection, int, or external convection, ext. The convective heat transfer coefficient depends on variables which affect the convective heat transfer, such as the geometry of the surface, fluid properties, fluid velocity and flow regimes. Determination of this parameter is therefore difficult and should be done experimentally. It should be noted that empirical correlations exist only for some types of fluid flow and simple geometries (e.g. Incropera et al., 2007; Çengel & Ghajar, 2011). However, experimental studies (e.g. Svec et al., 1983) show that the effect of heat transfer through convection between the fluid and the inside of the heat exchanger pipe, as well as the contact resistance on the outside of the pipe, are small compared to heat conduction within the pipe wall and the surrounding material, and therefore, can be assumed to be negligible for most applications involving GSES.

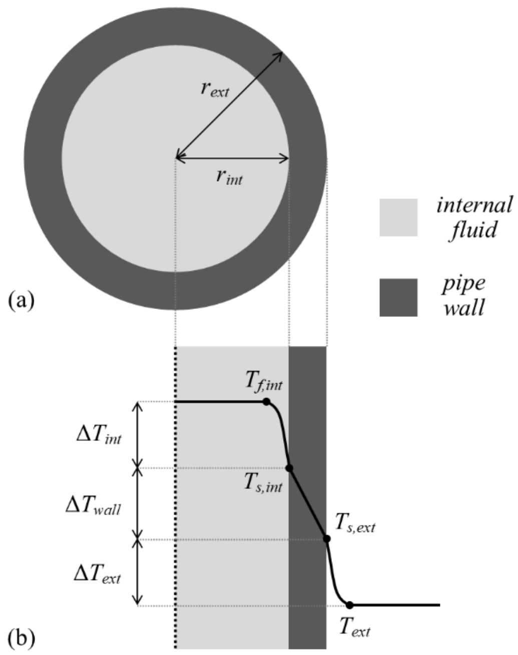

Figure 1 (a) plan view of a circular pipe, and (b) radial temperature distribution

Recent advances in numerical analysis have enabled the performance of such GSES to be studied with the aim of ensuring their safe operation and optimising their design. In order to simulate accurately the transfer of heat between these systems and the surrounding ground, the heat exchanger pipes must be included in the numerical model. However, due to the highly advective nature of the heat flux inside heat exchanger pipes, their modelling is often problematic.

Various methodologies for modelling the radial and axial heat transfer in GSES have been proposed in the literature. For example, Al-Khoury et al. (2005), Al-Khoury & Bonnier (2006) and Diersch et al. (2011b, 2011a) combined finite element (FE) analysis with Thermal Resistance and Capacity Models (TRCM), where a borehole containing heat exchanger pipes is represented as a single line in a three-dimensional (3D) FE model. The thermal interactions inside the borehole are modelled using the concept of thermal resistance, with the proposed expression for the thermal resistance between the pipes and the grout including conduction through the pipe wall, and convective heat transfer between the fluid and the inside of the pipe wall. In order to overcome numerical problems associated with modelling highly advective flows, Al-Khoury et al. (2005) and Al-Khoury & Bonnier (2006) adopted the Petrov-Galerkin FEM to solve the conductive-advective heat flux in heat exchanger pipes. Another family of TRCM, called Capacity Resistance Models (CaRM), was proposed by De Carli et al. (2010). Here, the equation of heat conduction in the surrounding soil was solved using the control volume approach.

The main disadvantage of the models based on the thermal resistance method is that each arrangement of the heat exchanger pipes in a borehole (i.e. single U-shaped, double U-shaped, coaxial, etc.) results in a different formulation. Additionally, there are uncertainties regarding the values of the thermal resistances of the various components as they are difficult to estimate accurately. For this reason, fully discretised FE models are often preferred due to their flexibility in simulating different pipe and borehole geometries, as well as boundary conditions.

Two-dimensional (2D) models of borehole heat exchangers consider only heat transfer within the cross-section of the borehole without accounting for the heat transfer along the pipes. For example, Zanchini & Terlizzese (2008), Lazzari et al. (2010) and Abdelaziz & Ozudogru (2016) performed analyses with COMSOL Multiphysics (COMSOL, 2012a) where solid elements were used to model the fluid in the pipes, the pipe wall and the surrounding material. The thermal conductivity of the pipe wall was modified to approximate the effect of the convective heat transfer on the inside of the pipe wall. These models provide only information on the temperature distribution within the cross-section of the borehole, rendering them impractical for the thermal design of GSES.

In order to simulate the heat transfer within the pipes whilst accounting for the GSES geometry and pipe configuration, 3D models are necessary. A common approach is to employ one-dimensional (1D) elements to simulate the flow of fluid and heat inside the heat exchanger pipes and use an algorithm based on the heat balance equation to couple them with the 3D solid elements for the surrounding material. The conduction of heat through the pipe wall, as well as the convective heat transfer on the inside and outside of the pipe wall may be included in the energy balance equation as heat sources/sinks. The heat flux calculated by the algorithm is then applied as a heat source or sink in the 3D domain. It must be noted that equations describing the convective heat transfer require the calculation of the temperature differences between the fluid inside the pipe, the pipe wall surfaces and the surrounding material (see Equation (1)). While the fluid temperature is obtained from the energy equation, the temperature in the 3D domain varies spatially (i.e. with distance from the heat exchanger pipes), meaning that an approximation must be made regarding the value of the surrounding temperature which is used to determine the heat flux between the pipe and the surrounding material.

3D simulations where the pipes were modelled with 1D elements using COMSOL Multiphysics and the above pipe-soil coupling methodology have been performed by Ozudogru et al. (2014), Batini et al. (2015), Bidarmaghz et al. (2016) and Caulk et al. (2016), amongst others. It must be noted that COMSOL Multiphysics avoids the numerical problems associated with highly advective flows by employing the artificial diffusion method (COMSOL, 2012b), which may affect the accuracy of the temperature solutions (Zienkiewicz et al., 2014). Cecinato & Loveridge (2015) analysed pipe-pile-soil interaction using ABAQUS (Dassault Systèmes, 2017) which solves the conductive-advective heat flux using the Petrov-Galerkin FEM with bilinear time-space shape functions proposed by Yu & Heinrich (1986, 1987).

The modelling approach adopted in the current paper is fundamentally distinct from those described in the abovementioned finite element studies. Firstly, the transient conductive-advective heat transfer along the pipes (modelled with 1D elements) is solved using the Petrov-Galerkin FEM which was shown by Cui et al. (2018a) and Gawecka et al. (2018) to produce accurate results, unlike other methods involving artificial diffusion or enhanced thermal conductivity. Secondly, heat transfer through convection between the fluid and the inside of the heat exchanger pipe, as well as the contact resistance on the outside of the pipe, is not included, since the definition of the input parameters for the pipe-soil coupling methodology (i.e. the convective heat transfer coefficient, see Equation (1)) and of the algorithm required to estimate the temperature in the material surrounding the pipe is problematic. In effect, as previously mentioned, available empirical data suggest that its effect on the overall heat transfer is expected to be limited.

This modelling approach is explored in this paper through a series of numerical analyses performed with the Imperial College Finite Element Program (ICFEP, Potts & Zdravković (1999)) which is capable of modelling fully coupled thermo-hydro-mechanical behaviour of porous materials (Cui et al., 2018b). Following a brief description of the FE formulation, numerical studies investigating the performance of 1D elements are presented and an effective method of simulating the heat transfer is proposed. The conclusions of these studies are then applied to the simulation of two thermal response tests (TRT). The excellent match between the measurements and numerical predictions demonstrates the validity of the chosen modelling approach.

Finite element method

Governing equations

Fluid and heat flow along heat exchanger pipe

One-dimensional incompressible fluid flow along a heat exchanger pipe is described by the continuity equation:

$$\frac{\partial v_f}{\partial l} = Q^f \tag{2}$$

where v_f is the fluid velocity, l is the pipe length and Q^f is any fluid source or sink.

Although the main modes of heat transfer include conduction, advection and radiation, the latter is considered to be negligible in heat exchanger pipes and is, therefore, disregarded in this formulation.

The equation governing one-dimensional heat transfer along a heat exchanger pipe is based on the law of conservation of energy, and can be written as:

$$\frac{\partial(\Phi_T dV)}{\partial t} + \frac{\partial Q_T}{\partial l} dV - Q^T dV = 0 \tag{3}$$

where t is time, Q_T is the total heat flux, Q^T represents any heat source/sink, dV is the infinitesimal volume and Φ_T is the heat content per unit volume which, when modelling the fluid inside the heat exchanger pipes, can be calculated as:

$$\Phi_T = \rho_f C_{pf}(T - T_r) \tag{4}$$

where ρ_f and C_{pf} are the density and specific heat capacity of the fluid, T is the fluid temperature and T_r is a reference temperature.

The total heat flux, Q_T, can be divided into two contributions: heat conduction, Q_d, and heat advection, Q_a, which are defined as:

$$Q_d = -k_T \frac{\partial T}{\partial l} \tag{5}$$

$$Q_a = \rho_f C_{pf} v_f (T - T_r) \tag{6}$$

where k_T is the thermal conductivity.

If the fluid is assumed to be incompressible, Equation (3) reduces to the transient heat conduction-advection equation:

$$\rho_f C_{pf} \frac{\partial T}{\partial t} + \rho_f C_{pf} v_f \frac{\partial T}{\partial l} - k_T \frac{\partial^2 T}{\partial l^2} = Q^T \tag{7}$$

The finite element formulation for coupled thermo-hydraulic problems is obtained by combining Equations (2) and (7). The θ-method time marching scheme has been adopted for solving the FE equations governing fluid and heat flow (Cui et al., 2018b). The detailed formulation for line (i.e. 1D) elements, which are employed to represent heat exchanger pipes, is presented in Gawecka et al. (2018). Note that in the original publication, these elements are referred to as 3D beam elements due to their possible use as structural elements. Although their mechanical response is not considered in this study, the same terminology will be used throughout this paper.

Heat transfer in surrounding medium

As the focus of the numerical studies presented in this paper is on the transfer of heat between the heat exchanger pipes and the surrounding material (i.e. borehole grout and soil mass), the flow of pore water in the soil was not considered, while heat radiation was assumed to be negligible (Farouki, 1981). Therefore, only the conduction of heat was modelled.

The multi-dimensional heat transfer equation based on the law of conservation of energy is given by:

$$\frac{\partial(\Phi_T dV)}{\partial t} + \nabla \cdot \{Q_T\} dV - Q^T dV = 0 \qquad (8)$$

where, for fully saturated soil, Φ_T is defined as:

$$\Phi_T = \left(n\rho_f C_{pf} + (1-n)\rho_s C_{ps}\right)(T - T_r) \qquad (9)$$

where n is the porosity, ρ_f and ρ_s are the densities of the pore fluid and solid particles, respectively, whereas C_{pf} and C_{ps} are the specific heat capacities of the pore fluid and solid particles, respectively.

As the effect of heat advection in the soil is neglected in this study, the total heat flux $\{Q_T\}$ is equal to the conductive heat flux:

$$\{Q_T\} = \{Q_d\} = -[k_T]\{\nabla T\} \qquad (10)$$

where $[k_T]$ is the thermal conductivity matrix.

Assuming that that the soil is rigid, Equation (8) simplifies to the transient heat conduction equation:

$$\left(\rho_f C_{pf} + (1-n)\rho_s C_{ps}\right)\frac{\partial T}{\partial t} - \nabla \cdot ([k_T]\{\nabla T\}) = Q^T \qquad (11)$$

Again, the θ-method time marching scheme has been employed for solving Equation (11). The detailed formulation for solid elements, which are used to model the soil domain, can be found in Cui et al. (2018b).

Finite element implementation

In geotechnical engineering, the most widely used finite element method is the Galerkin FEM. Although it has been successfully employed to simulate a variety of geotechnical problems, it has been shown to produce erroneous solutions when dealing with problems where advection dominates heat transfer. In such cases, the temperature distribution computed with Galerkin FEM exhibits unrealistic oscillations, the magnitude of which increases with increasing Péclet number, Pe, (e.g. Donea & Huerta, 2003, Al-Khoury, 2012, Zienkiewicz et al., 2014, Cui et al., 2016). The Péclet number describes the ratio between the advective and conductive heat fluxes and is defined as:

$$Pe = \frac{\rho_f C_{pf} v_f L}{k_T} \tag{12}$$

where L is the characteristic length, which, in the case of the finite element method, is the element length in the direction of fluid flow. A possible form of eliminating the abovementioned oscillations is to reduce the Péclet number to 1 if elements with linear shape functions are used, or 2 if quadratic elements are adopted (Cui et al., 2016). However, in a problem with fixed fluid properties and fluid velocity, this is only possible by refining the finite element mesh (i.e. reducing L), resulting in a very large number of extremely small elements. This is certainly the case for heat exchanger pipes where fluid velocities are high, making their simulation with the Galerkin FEM computationally expensive. For example, achieving a Péclet number of 1 in a problem where water flows through a pipe at a velocity of 0.34 m/s (as in one of the case studies considered in Section 0) requires an element length of 4.3×10^{-7} m, which equates to over 2.3×10^{6} elements per metre of pipe.

In order to overcome this problem and allow greater values of Péclet number to be used in the numerical analysis, Petrov-Galerkin FEM has been proposed (e.g. Brooks & Hughes, 1982, Zienkiewicz et al., 2014). Unlike the Galerkin FEM, where the interpolation functions are identical to the weighting functions, the Petrov-Galerkin FEM weights the upstream node more heavily than the downstream one, which is achieved by employing weighting functions which are different from the interpolation functions. Although several weighting functions have been reported in the literature (e.g. Christie et al., 1976, Huyakorn, 1977, Ramakrishnan, 1979, Dick, 1983, Westerink & Shea, 1989), it was found that only some functions, together with a correct implementation, result in accurate solutions to problems involving an advection-dominated heat flux (Brooks & Hughes, 1982, Cui et al., 2018a). In the current study, the Petrov-Galerkin FEM proposed by Cui et al. (2018a) was used for solving the equation governing the heat transfer along heat exchanger pipes (Equation (7)). Its detailed formulation, as well as a demonstration of its effectiveness, can be found in Cui et al. (2018a) and Gawecka et al. (2018). It should be noted that the conventional Galerkin FEM was adopted for solving the equations of fluid flow along heat exchanger pipes (Equation (2)) and conductive heat transfer in solid elements (Equation (11)).

Development of a modelling approach

This section investigates the performance of the 3D beam elements when used to represent a single heat exchanger pipe embedded in soil, with the obtained results being used to establish an accurate 3D modelling approach for this type of problem. Two distinct sets of studies are carried out, with the first of these focussing on the interaction between a heat exchanger pipe and the surrounding medium without including the effect of the pipe wall, in an effort to simplify the problem being analysed. Subsequently, a second set of studies is performed investigating the impact of the presence of the pipe wall and how it can be efficiently included in the developed modelling approach.

The problem analysed in this section involves a single 30 m long vertical heat exchanger pipe installed in the centre of a cylindrical mass of soil as illustrated in Figure 2(a). Although this is a simplified problem with a rotational symmetry, it allows the development of a modelling approach which employs 3D beam elements and subsequently can be used to simulate any heat exchanger pipe arrangement. Two methodologies for modelling this coupled thermo-hydraulic problem were employed:

- “beam” analysis – in this case, the water inside the pipe is represented using 3D beam elements (where 1D fluid and heat flow are described by Equations (2) and (7), respectively) placed at the axis of symmetry of the problem as shown in Figure 2(b). It should be noted that although the 3D beam elements are zero-thickness elements (in terms of their geometry in the FE mesh), a cross-sectional area is assigned to them as a property to allow for the computation of the heat capacity and volumetric fluid flow. The 3D beam elements are 2-noded with linear fluid pressure and temperature shape functions, whereas the solid elements discretising the soil are 8-noded hexahedra with linear temperature shape functions (only one quarter of the domain was modelled due to symmetry). As described previously, the use of Petrov-Galerkin FEM was limited to the solution of the heat transfer equation within the line elements.

- "solid" analysis – the water inside the pipe is discretised with solid elements with a radius equal to that of the modelled pipe (see Figure 2(c)) meaning that no 3D beam elements were used. Therefore, taking advantage of the rotational symmetry of the problem, 2D axisymmetric analyses were performed in this case, which are computationally more efficient than full 3D analyses. The solid elements are 4-noded with linear fluid pressure and temperature shape functions allowing for simulation of heat conduction and advection. Clearly, in this case, the Petrov-Galerkin FEM for solid elements (see Cui et al. (2018a) for more details) was required for the solution of the heat transfer equation within the pipe. The surrounding soil was discretised by 4-noded quadrilateral elements with linear temperature shape functions.

A no heat flux boundary condition was prescribed at all mesh boundaries except for the far vertical boundary where the temperature was not allowed to change from its initial value of 15 °C. Water was injected into the pipe at a constant rate of 5×10^{-5} m^3/s with its inlet and outlet being located at the top and bottom of the mesh, respectively. A constant temperature of 30 °C was prescribed at the inlet and the coupled thermo-hydraulic boundary condition, which applies a heat flux equivalent to the energy associated with the fluid flowing across the boundary, was applied at the outlet (see Cui et al. (2016) for further details on this nonlinear boundary condition). Naturally, in the axisymmetric analyses, the inflow and outflow of water, as well as the thermo-hydraulic boundary condition, were applied over the line defining the radius of the pipe.

The effect of pipe diameter was investigated by changing the cross-sectional area of the 3D beam elements or adjusting the finite element mesh in the analyses where the water inside the pipes was modelled with solid elements. In this study, internal pipe diameters of 10 mm (D10), 20 mm (D20), 30 mm (D30) and 40 mm (D40) were considered, covering the range of typical diameters of heat exchanger pipes. As the water flow rate was the same in all analyses, the water velocity, and hence the Péclet number, was different for the four pipe diameters. In the vertical direction, the mesh was divided into 30 elements with a height of 1 m, resulting in a Péclet number in the pipe ranging from approximately 277,000 for a pipe diameter of 40 mm to 4.4 million for a pipe diameter of 10 mm, justifying the need to use Petrov-Galerkin FEM. The 3D beam elements, as well as the solid elements representing the water inside the pipe, were modelled with properties of water, whereas properties of soil were used for the surrounding solid elements. All relevant material properties are listed in Table 1.

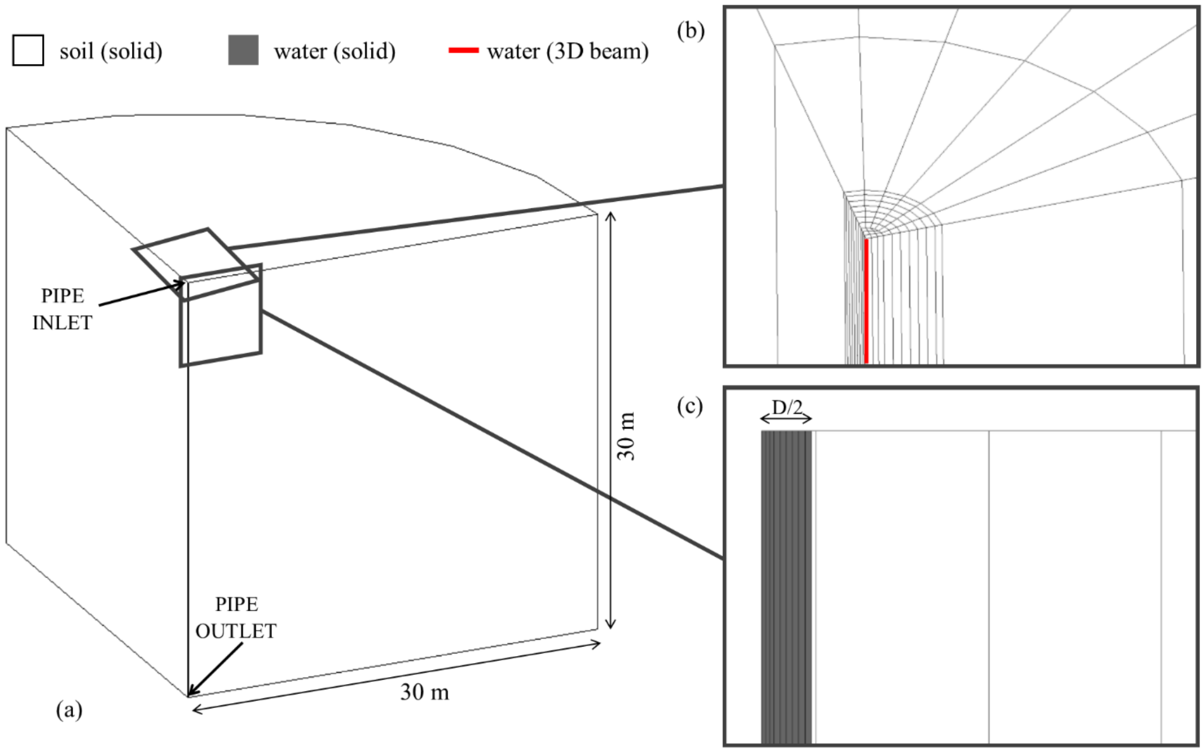

Figure 2 (a) geometry of the problem (b) detail of mesh with pipe represented as 3D beam elements, and (c) detail of mesh with pipe modelled with solid elements

Table 1 Material properties for single pipe analyses

	Water	Soil
Volumetric heat capacity, ρC_p (kJ/m^{3}K)	4180	3080
Thermal conductivity, k_T (W/mK)	0.6	2.0

Simulating a single pipe without the pipe wall

Firstly, the problem described above was simulated without accounting for the effect of the pipe wall. Figure 3 compares the outlet temperature evolution in an analysis where the pipe was modelled with 3D beam elements (denoted ‘beam’) and in an analysis where the water inside the pipe was discretised with solid elements (denoted ‘solid’). In both analyses, the internal pipe diameter was 40 mm. Clearly, solid elements are capable of simulating the three-dimensional temperature variation inside the pipe (i.e. along the length of the pipe and within its cross-section), where the outside edge of the pipe is always at a lower temperature than the centre as it transfers heat to the surrounding soil. Hence, Figure 3 plots the outlet temperature measured at the centre of the pipe, at the edge of the pipe, as well as the average water temperature at the outlet. Due to the one-dimensional nature of the 3D beam element, simulating this variation of temperature within the cross-section of the pipe is not possible. The results in Figure 3 show that in the ‘beam’ analysis, the outlet temperature is significantly higher than the average outlet temperature in the ‘solid’ analysis, although the two appear to converge in the long term. The reason for this is that the 3D beam elements are zero-thickness elements and cannot simulate the actual contact area between the pipe and the soil, hence underestimating the heat transfer rate between the pipe and the soil.

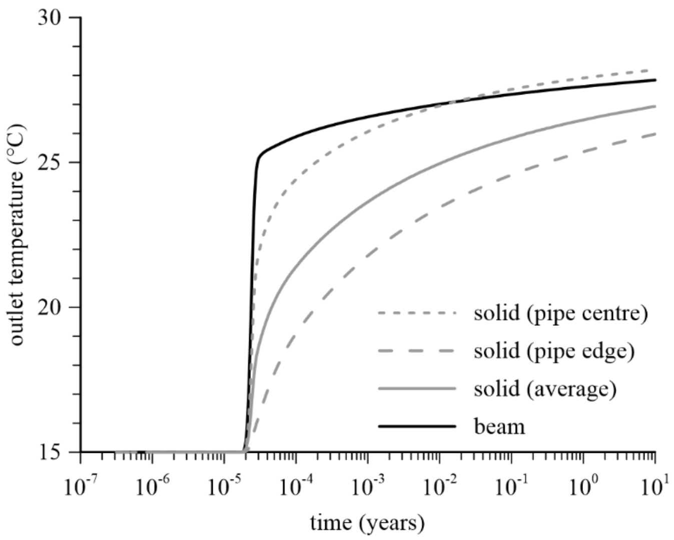

Figure 3 Outlet temperatures in the pipe modelled with solid elements and beam elements for a pipe diameter of 40 mm

Although modelling the water inside the pipes with solid elements simulates the behaviour of heat exchanger pipes more realistically, it is computationally more expensive as it requires these elements to have fluid pressure degrees of freedom. Simulating the water flow inside the pipes with 3D beam elements reduces substantially the required number of degrees of freedom. Furthermore, the modelling approach using solid elements requires the Petrov-Galerkin FEM for 2D or 3D, the implementation of which is more complex than that for 1D elements, especially in problems where the direction of fluid flow changes, generating large velocity gradients (Cui et al., 2018a). However, Figure 3 clearly demonstrates that the direct use of 3D beam elements should be avoided when the thermal performance of a heat exchanger needs to be simulated accurately, as such methodology tends to underestimate heat transfer from the heat exchanger pipes to the surrounding medium.

Therefore, an alternative approach to simulate this type of problems is required. Such an approach would have to satisfy a number of modelling requirements: the heat flux should be advection-dominated and the radial heat transfer to the surrounding soil should be reproduced accurately. The latter implies that both the contact area between the pipe and soil and the interaction mechanisms between the two, which result in a non-uniform radial temperature distributions within the pipe (see Figure 3), must be accounted for. As part of this research, a number of possible strategies have been considered:

a) A large thermal conductivity value was assigned to the volume corresponding to the pipe to enhance heat flux along its axis without simulating fluid flow. However, this does not allow the fundamental aspects of advection-dominated heat flux to be simulated.
b) Zero-thickness beam elements in a 2D axisymmetric analysis or zero-thickness shell elements in a 3D analysis, through which the fluid flows, were placed at the radial distance corresponding to the edge of the pipe. Although this allows the simulation of the correct contact area between the pipe and the soil, it fails to replicate the non-uniform temperature distributions within the pipe resulting in an overestimation of the radial heat transfer to the soil.
c) Another approach that allows the modelling of the correct contact area is to leave a cavity in the finite element mesh of the same shape, size and location as that of the pipe, place 3D beam elements along the centre line of the cavity to represent the pipe and subsequently tie the

temperature degrees of freedom of the nodes of the beam element to those around the edge of the cavity (i.e. soil nodes) at the same elevation. This results in a behaviour very similar to that of approach (b), hence overestimating the radial heat transfer to the soil. A possible solution to this would be to introduce a ratio between the temperature at the 3D beam nodes and those at the edge of the cavity. However, an inspection of the results obtained in the 'solid' analysis described previously showed that such a ratio is difficult to define as it varies along the pipe and with time.

Given the clear shortcomings of the modelling approaches described above, an alternative is proposed here whereby 3D beam elements are combined with the use of a new material, which is termed the Thermally Enhanced Material (TEM) and is discretised with solid elements. The TEM is placed around the 3D beam elements (see Figure 4) and has the same cross-sectional area as the water inside the pipe, meaning that the same contact area between the water moving inside the pipe and the surrounding medium as in the actual problem can be modelled. Since only heat conduction is considered inside the TEM, it does not require pore fluid pressure degrees of freedom, reducing the computational effort and complexity compared to the approach where the solid elements simulate the flow of water. Furthermore, by controlling the thermal properties of the TEM, it is possible to increase the radial heat transfer rate between the 3D beam and the soil such that a more realistic response of the pipe is simulated.

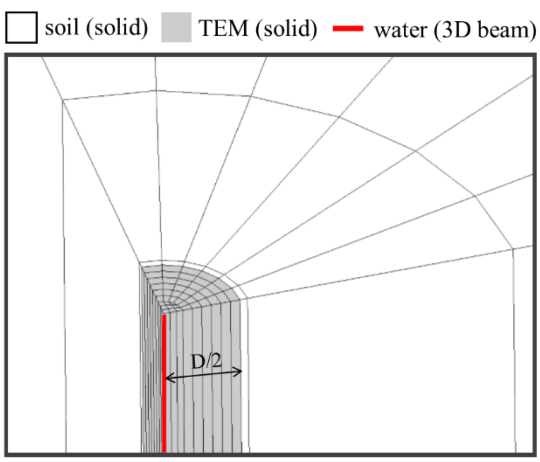

Figure 4 Detail of the finite elements mesh with pipe modelled with 3D beams and the TEM modelled with solid elements

As part of this research, an extensive numerical study was performed with the aim of determining the appropriate thermal properties of the TEM. The volumetric heat capacity of the TEM ($\rho {C_p}_{TEM}$) was set to 1 kJ/m^{3}K, as the heat capacity of the fluid is already included in the formulation of the 3D beam element (see Equation (7) and Gawecka et al. (2018) for further details on the implementation of this type of elements), whereas its thermal conductivity (k_{TEM}) was varied until the outlet temperature of the 3D beam matched the average outlet temperature computed in the 'solid' analysis (see Figure 3). This ensures that the same amount of energy is being transferred from the heat exchanger pipe to the surrounding medium. The results of this study on a pipe with internal diameter of 40 mm are plotted in Figure 5. It is clear that, as k_{TEM} increases, the heat transfer rate increases, reducing the outlet temperature. The value of k_{TEM} which produced the best response was found to be 10 W/mK. It can be seen in Figure 5 that, for this value of k_{TEM}, the difference in temperature between the "solid" and the "beam" analyses is very small and limited to a very narrow interval of time. In effect, for time instants above 3 × 10^{-4} years (2.6 hours), no discernible difference exists.

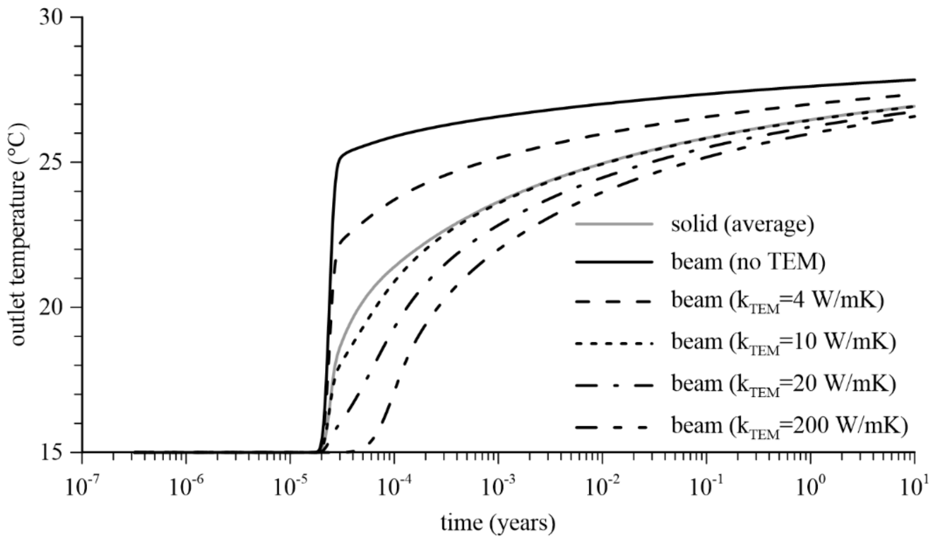

Figure 5 Effect of thermal conductivity of the TEM on the outlet temperature for a pipe diameter of 40 mm

The same procedure was then repeated for pipes with internal diameters of 30, 20 and 10 mm. In all cases, it was found that k_{TEM} of 10 W/mK gave the best reproduction of the average outlet temperature. These results are plotted in Figure 6, which confirms the conclusions drawn for the larger diameter pipe, with the temperature differences being more pronounced in the very short term. However, it should be noted that the maximum temperature difference recorded in all cases was limited to 1.2 °C for D10 for a rather short duration and in the very short term (less than 10^{-5} years or 5 minutes), suggesting an excellent agreement between the developed modelling approach with k_{TEM} of 10 W/mK and the results obtained when the water is explicitly modelled using solid elements.

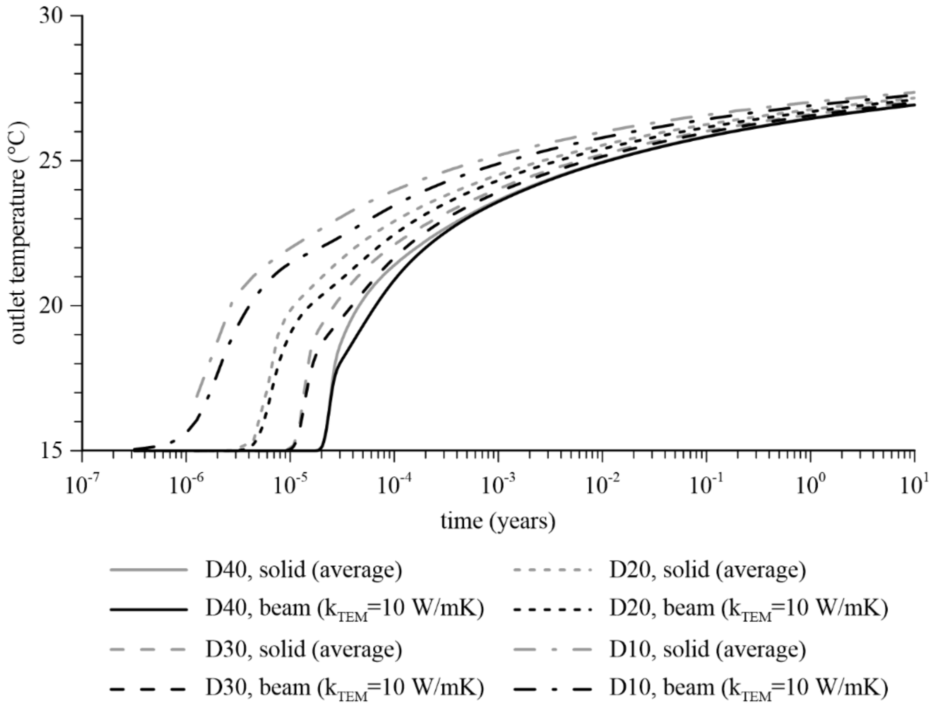

Figure 6 Outlet temperatures in pipes with different diameters modelled with solid elements and the new approach with k_{TEM}*=10 W/mK*

Table 2 Details of studies performed to investigate the properties of the TEM

Study	Details	Outcome
Effect of thermal conductivity of TEM	Thermal conductivity of TEM varied	k_{TEM} = 10 W/mK
Effect of pipe diameter	Pipe diameters studied: 10 mm, 20 mm, 30 mm, 40 mm	k_{TEM} = 10 W/mK independently of pipe diameter
Effect of fluid flow rate	Fluid flow rate varied between 2.5×10^{-5} m^3/s and 10×10^{-5} m^3/s	k_{TEM} = 10 W/mK independently of fluid flow rate
Inlet temperature	Inlet temperature varied between 0 and 45 °C	k_{TEM} = 10 W/mK independently of inlet temperature

Effect of soil thermal conductivity	Thermal conductivity of soil varied between its extremes of 0.5 and 4 W/mK (VDI, 2010)	k_{TEM} = 10 W/mK independently of soil thermal conductivity
Effect of soil volumetric heat capacity	Volumetric heat capacity of soil varied between 2080 and 4080 kJ/m^{3}K	k_{TEM} = 10 W/mK independently of soil volumetric heat capacity

Additional studies investigating a number of variables were also performed as part of this research. Although the results are not presented here for brevity, their details and outcomes are summarised in Table 2. The key conclusion is that a k_{TEM} of 10 W/mK was shown to produce the most satisfactory results in all cases investigated.

Simulating the effect of the pipe wall

The second set of studies aimed at investigating the effect of heat conduction through the heat exchanger pipe wall. This was achieved by firstly performing numerical analyses where the water inside the pipe is modelled with solid elements. In order to include the effect of the pipe wall, the finite element mesh shown in Figure 2(c) was altered by adding a single 3 mm wide column of 4-noded solid elements with linear temperature shape functions between the water and the soil. Thermal properties of high density polyethylene (HDPE, ρC_p of 1800 kJ/m^{3}K and k_T of 0.4 W/mK), which is typically used for heat exchanger pipes, were assigned to these elements.

Figure 7 compares, for all the considered pipe diameters, the average outlet temperature computed in these analyses with those previously obtained without the pipe wall. It can be seen that, as expected, the inclusion of the pipe wall results in a lower heat transfer rate and, therefore, a higher outlet temperature. This response is attributed to the considerably lower thermal conductivity of HDPE when compared to that of the surrounding soil, which slows down the heat transfer from the pipe fluid to the soil. Furthermore, since the thermal resistance of a thin wall cylinder decreases with increasing radius (Incropera et al., 2007; Çengel & Ghajar, 2011), the effect of the pipe wall is greater for the smaller diameter. The maximum temperature differences due to the presence of the wall are 2.8, 3.3, 4.0 and 6.3 °C for D40, D30, D20 and D10, respectively. However, it should be noted that these differences between the two cases occur in the short term (at times less than 2.8 × 10^{-5} years or 15 minutes) and reduce with time for all pipe diameters.

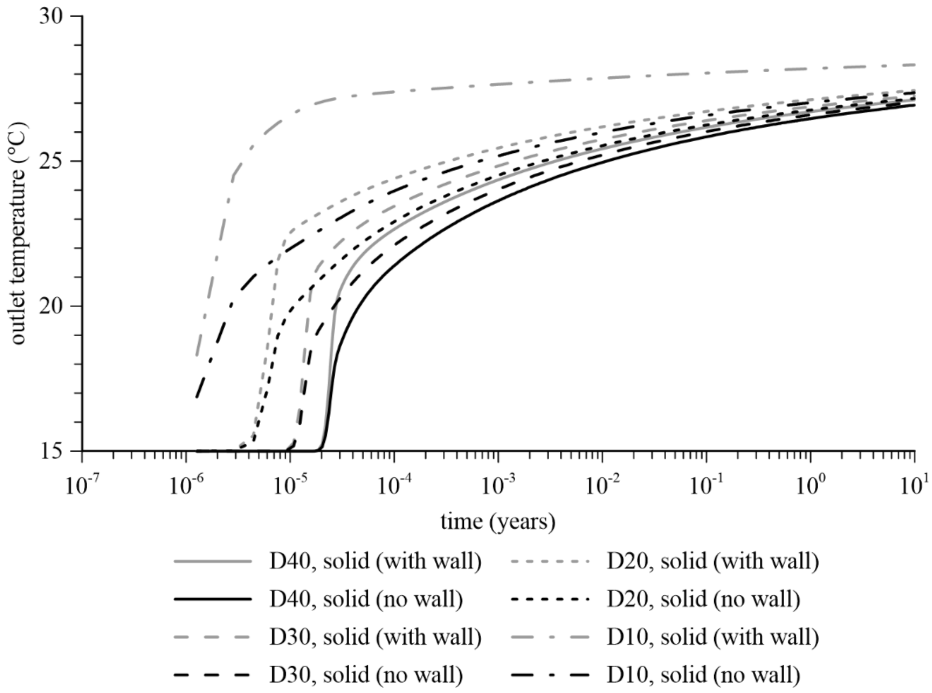

Figure 7 Comparison of average outlet temperatures in analyses with and without the pipe wall

Once the effect of the pipe wall was established, the analyses were repeated with the new modelling approach which employs 3D beam elements and the TEM. Clearly, using k_{TEM} of 10 W/mK would not be able to reproduce the response of the pipe with the wall shown in Figure 7 and a lower k_{TEM} is required to simulate the lower heat transfer rate arising from the lower thermal conductivity of the pipe wall. Therefore, the appropriate value of k_{TEM} was again established by conducting a parametric study. Figure 8 plots the outlet temperatures obtained with this approach and the values of k_{TEM} which produced the best match with the "solid" analyses, which range from k_{TEM} of 1 W/mK for D10 to k_{TEM} of 6 W/mK for D40. It can be seen that the temperature differences between the two sets of analyses are very small, with a maximum value of 1.4 °C occurring at times less than 4 × 10^{-5} years (or 21 minutes) and becoming practically non-existent after 3 × 10^{-4} years (or 2.6 hours).

Unlike in the study presented in Section 3.1, where a single value of k_{TEM} (10 W/mK) was found to be suitable for all pipe diameters, including the effect of the pipe wall requires a different value of k_{TEM} for each diameter. The results of this study are summarised in Figure 9 which plots the obtained value of k_{TEM} for each pipe diameter considered. It can be seen that the established variation of k_{TEM} with the diameter of the pipe (D) is perfectly reproduced using a simple logarithmic relationship ($R^2 = 1.0$):

$$k_{TEM} = 3.62\ln(D) - 7.33, \qquad 10\,mm \le D \le 40\,mm \tag{13}$$

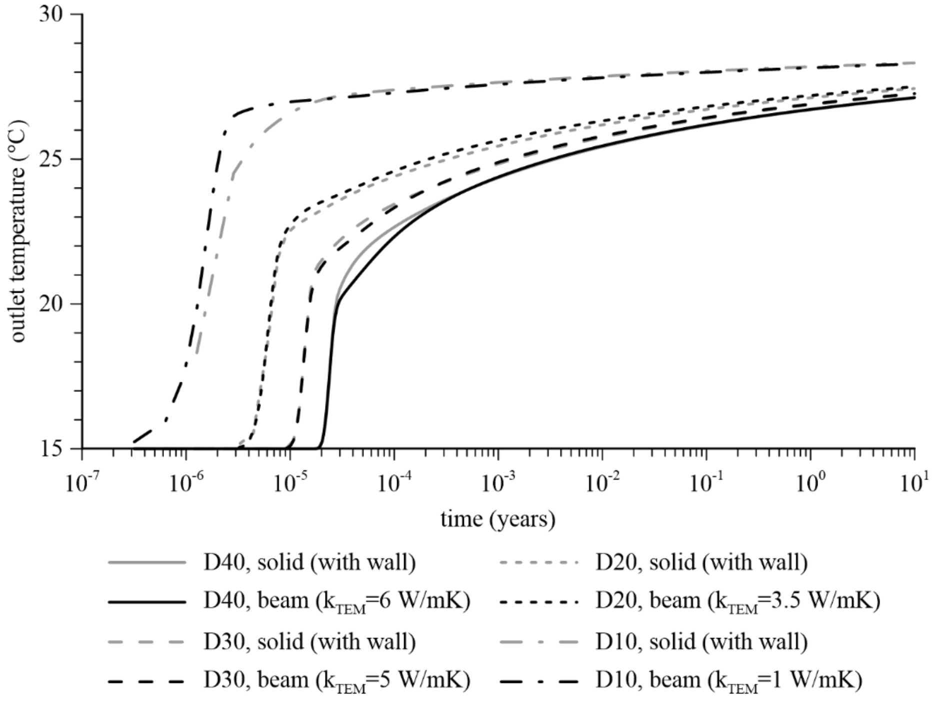

Figure 8 Outlet temperatures in pipes with different diameters modelled with solid elements and the new approach with different values of k_{TEM}

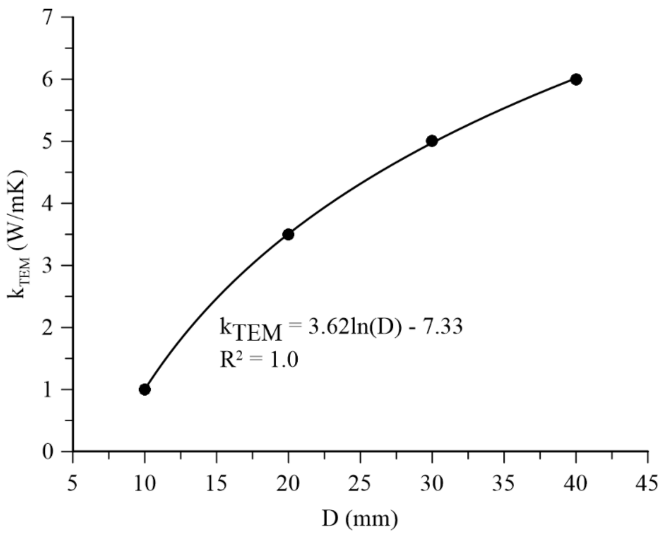

Figure 9 Empirical relationship between the internal pipe diameter (D) and k_{TEM} for modelling the effect of pipe wall

It should be noted that this empirical expression was obtained for a specific pipe with a wall thickness of 3 mm and thermal properties of HDPE. While this study should be repeated if different pipe wall thickness and/or material are considered, the characteristics chosen here are typical for pipes used as heat exchanger pipes and are the same as those in the thermal response tests simulated in Section 0.

Verification of the modelling approach

Thermal response tests

A thermal response test (TRT) is a field test used to determine the soil's thermal conductivity, as well as to estimate the borehole's thermal resistance (Loveridge et al., 2014). This is achieved by pumping a heated fluid (usually water) around a loop of heat exchanger pipes placed in a borehole. The flow rate and the temperature of the fluid at the inlet and outlet are monitored throughout the test, while the power used to heat the injected fluid is controlled. Hence, thermal conductivity can be calculated based on the energy transferred to the soil, obtained from the temperature difference between the inlet and the outlet, assuming that the borehole heat exchanger acts as an infinite line source. In this paper, two TRTs performed under considerably different conditions – laboratory (Beier et al., 2011) and field (Loveridge et al., 2014) – have been simulated numerically in order to validate the proposed modelling approach, which uses 3D beam elements and the TEM to model the response of heat exchanger pipes.

Laboratory TRT (Beier et al., 2011)

Beier et al. (2011) performed a TRT on a borehole heat exchanger under laboratory conditions where an 18 m long aluminium tube with a diameter of 126 mm served as the borehole wall and was placed in the centre of a 1.8 m x 1.8 m x 18 m box filled with saturated sand. The borehole contained a single U-tube heat exchanger pipe and was filled with bentonite grout mixed with water. The heat exchanger pipe had an internal diameter of 27.33 mm, a wall thickness of 3 mm and was made of HDPE. The centre-to-centre spacing between the two legs of the pipe was 53 mm. During the test, the water was circulated through the pipe at a rate of 0.197 l/s (1.97×10^{-4} m^3/s), corresponding to a fluid velocity of 0.34 m/s. Thermistors were used to monitor the inlet and outlet temperatures (plotted in Figure 10), as well as the temperature at various locations inside the sandbox. These thermistors recorded a temperature of approximately 22 °C prior to the test which was assumed to be the initial temperature in the numerical analyses.

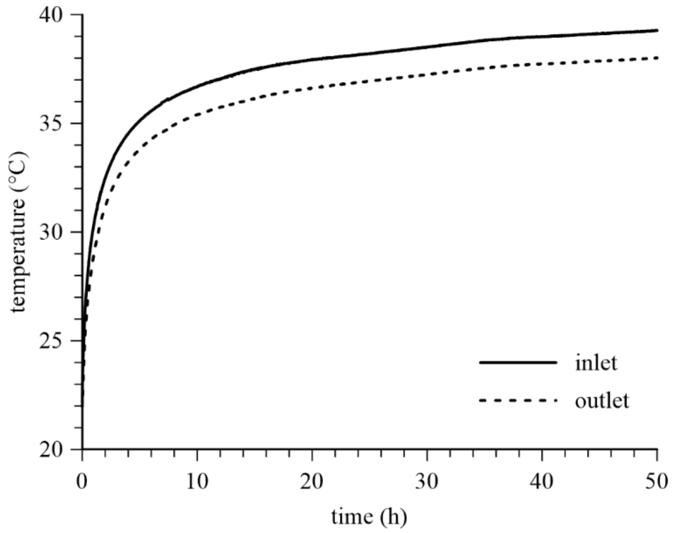

Figure 10 Inlet and outlet fluid temperatures in the borehole TRT (data from Beier et al., 2011)

Field TRT (Loveridge et al., 2014)

The second TRT considered in this study was carried out at a development site in central London and reported by Loveridge et al. (2014). A single U-tube heat exchanger pipe was installed to 26 m depth in a borehole which was then backfilled with C35 hard pile cementitious grout. The diameter of this pile was 300 mm over the top 26.8 m and 200 mm below that to an unknown depth. The two legs of the pipe were separated evenly with a centre-to-centre spacing of 135 mm. The pipe had an internal diameter of 26.2 mm, a wall thickness of 2.9 mm and was made of high performance polyethylene ‘PE100’, which has the same thermal conductivity compared to HDPE. The entire length of the pile was within London Clay, with the groundwater level 4 m below the top of the pile. Water was used as the circulation fluid. Throughout the test, the flow rate was measured using an electromagnetic flow meter, whereas thermocouples were used for the fluid temperature measurements. Additionally, vibrating wire strain gauges (VWSG) provided temperature monitoring at selected points within the grout. It should be noted that the data from the VWSG sensors was published later by Cecinato & Loveridge (2015).

The undisturbed ground temperature of 17.7 °C was obtained from the initial circulation stage. This value was assumed to be constant spatially and was used as the initial temperature in the numerical analyses. Loveridge et al. (2014) provide the time series of flow rate, Q_f, applied power, Q, and mean fluid temperature, T_{av}, throughout the test. The latter two are calculated using:

$$Q = \rho_f C_{pf} Q_f (T_{in} - T_{out}) \tag{14}$$

$$T_{av} = \frac{1}{2}(T_{in} + T_{out}) \tag{15}$$

where T_{in} and T_{out} are the measured temperatures at the inlet and the outlet of the pipe, respectively. When reproducing the TRT numerically, T_{in} is applied as a boundary condition at the inlet of the pipe, whereas the measured T_{out} is compared with the computed T_{out}. Hence, the measured T_{in} and T_{out}, which were not made available in the published literature, were calculated by solving Equations (14) and (15) simultaneously. It should be noted that a constant flow rate of approximately 371.7 l/h (1.032 × 10^{-4} m^3/s) was measured, corresponding to a fluid velocity of 0.19 m/s, with a volumetric heat capacity of 4180 kJ/m^3°C being assumed for water. The obtained inlet and outlet temperatures during the different stages of the test are presented in Figure 11.

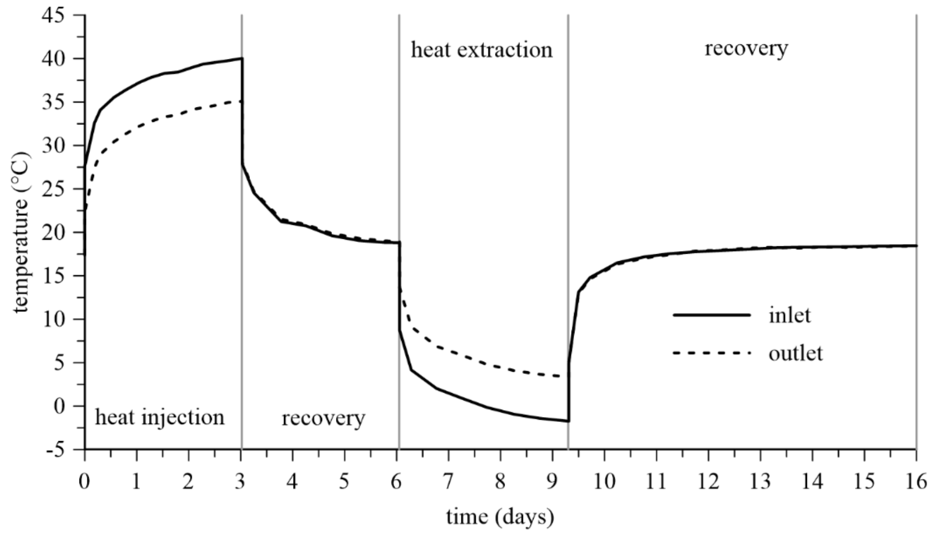

Figure 11 Inlet and outlet fluid temperatures in the field TRT (calculated from data from Loveridge et al., 2014)

Numerical modelling

Figure 12 shows the 3D finite element meshes used for simulation of the laboratory TRT by Beier et al. (2011) and the field TRT by Loveridge et al. (2014). The mesh for the former has the same dimensions as the sandbox (i.e. 1.8 m x 1.8 m x 18 m). In the case of the field TRT, the mesh extends to 30 m depth, with the pile modelled as having a uniform diameter of 300 mm, whereas the lateral cylindrical boundary of the mesh is located at a radial distance of 5 m from the centre of the borehole. Due to symmetry, only half of the problem was discretised in both studies. The heat exchanger pipes, which are U-shaped with inlet and outlet at the top of the mesh and a horizontal connection at the bottom of the borehole, were modelled using 2-noded 3D beam elements which had a temperature and fluid pressure degrees of freedom at all nodes, whereas the surrounding materials (TEM, grout and soil) were discretised with 8-noded hexahedral solid elements with only temperature degrees of freedom at all nodes. The position of the 3D beam elements corresponds to the axis of the heat exchanger pipes in the tests, whereas the cross-sectional area of the TEM, similar to the analyses presented in Section 0, corresponds to that of the inside of the pipes employed in the tests, i.e. the region discretising the TEM has a radius of 13.67 mm and 13.1 mm, respectively, for the lab and field test.

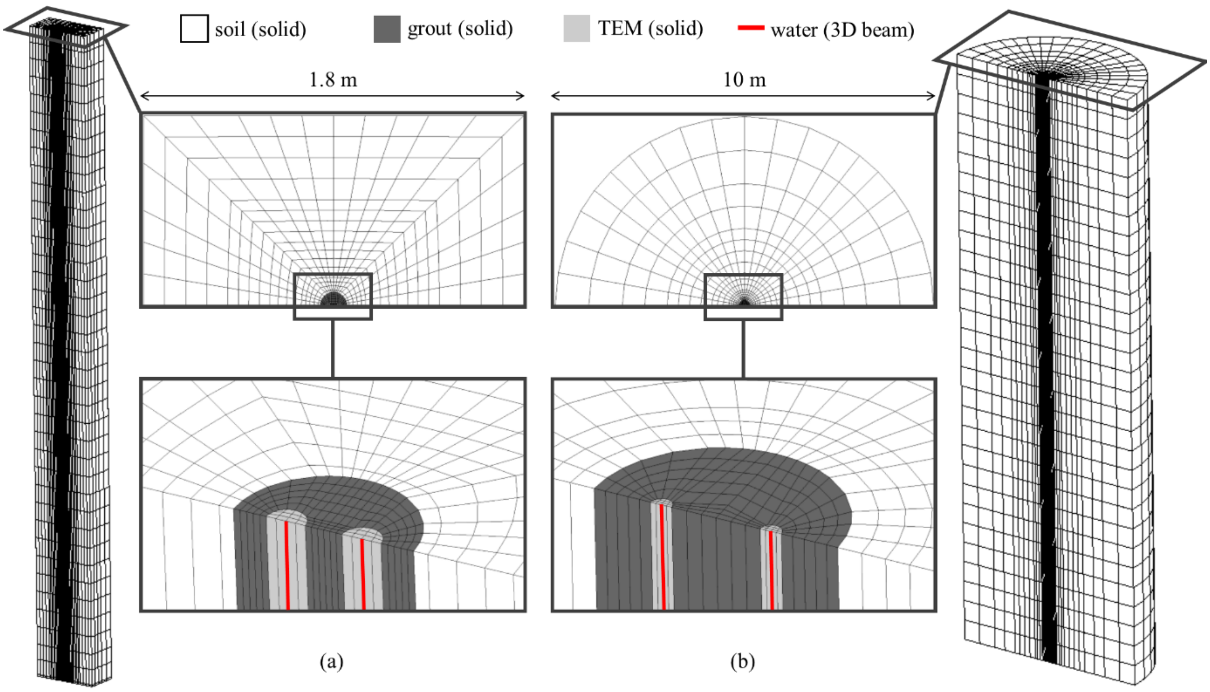

Figure 12 Finite element meshes used for simulation of: (a) the laboratory TRT, and (b) the field TRT

As in both cases only half of the problem was modelled, the flow rate prescribed at the pipe inlet was half of the actual flow rate – 9.85 × 10^{-5} m^3/s in the laboratory TRT and 5.16 × 10^{-5} m^3/s in the field TRT. Similarly, the 3D beam elements were assigned with a cross-sectional area which was half of the fluid flow area in the actual pipes. The thermal boundary conditions included applied temperature at the pipe inlet which was the same as that measured in the tests (see Figure 10 and Figure 11), and the coupled thermo-hydraulic boundary condition (Cui et al., 2016) at the pipe outlet. In the laboratory TRT set-up, the top and bottom of the sandbox were insulated whereas the sides were maintained at a constant temperature, since it was reported that air was circulated continuously through a guard space (Beier et al., 2011). In the numerical analyses, this set up was simulated by applying a no heat flux boundary condition at the ends and no change in temperature on the sides. In the field TRT, no change in temperature was allowed at all mesh boundaries, with the exception of the plane of symmetry, where a no heat flux boundary condition was prescribed.

Table 3 Material properties for reproduction of the TRTs

	Volumetric heat capacity, ρC_p (kJ/m^{3}K)	Thermal conductivity, k_T (W/mK)
Water	4180 [1]	0.6 [1]
TEM	1 [4]	10 / 4.5 [4]
Laboratory TRT		
Grout	3900 [1]	0.73 [2]
Soil	2500 [1]	2.82 [2]
Field TRT		
Grout	1800 [1]	2.0 [1]
Soil	2150 [3]	2.4 [3]

[1] VDI (2010); [2] Beier et al. (2011); [3] Loveridge et al. (2014); [4] this study

The thermal properties of all materials are listed in Table 3. Beier et al. (2011) measured the thermal conductivity of the saturated sand and the bentonite grout using a non-steady-state thermal probe. The thermal conductivity of the ground in the field TRT is that calculated by Loveridge et al. (2014) from the results of the TRT, whereas the adopted volumetric heat capacity of the ground is the same as that assumed by Loveridge et al. (2014). All other material properties were obtained from the literature

(VDI, 2010). The thermal properties of TEM are based on the conclusions of the numerical studies presented in Section 0. In order to investigate the effect of the proposed modelling approach, three analyses for each TRT were performed – one with k_{TEM} of 10 W/mK which excludes the effect of the pipe wall, one with k_{TEM} of 4.5 W/mK which was calculated using Equation (13) and includes the effect of the pipe wall, and one where no TEM is used.

Results

Figure 13 and Figure 14 compare the evolution of the outlet temperature recorded in the laboratory TRT and the field TRT, respectively, with the outlet temperature obtained from the three numerical analyses with k_{TEM} of 10 W/mK, 4.5 W/mK and no TEM. Furthermore, the study performed by Beier et al. (2011) involved extensive monitoring of the temperature in the sand surrounding the borehole. Thermocouples were installed in a grid in the plane which runs through the centrelines of the two legs of the U-tube, on the side of the borehole that has the inlet leg of the U-tube. The locations of the thermocouples are illustrated in Figure 15 together with measured and predicted temperatures histories. Note that these are the average temperature of the four thermocouples located at the same distance away from the borehole wall (d) but at different depths, with the exception of the average measurements at the borehole wall where thermocouple number 15 was excluded as it appeared to show anomalously high temperatures. Lastly, Figure 16 presents the measured and computed temperature histories at two monitoring points within the grout in the field TRT which were positioned at a distance of 30 mm away from the centre of the pile, directly between the two pipe legs (as depicted in Figure 16) and at depths of 13.8 m and 23.8 m, respectively.

In terms of the outlet temperature (Figure 13 and Figure 14), the analyses with k_{TEM} of 10 W/mK and 4.5 W/mK give very similar results and both reproduce the two TRTs very well, with the predicted differences in temperature being limited to 0.8 °C for the field TRT and only 0.2 °C for the laboratory TRT. Conversely, the analyses where the TEM was not included underestimate the heat transfer between the pipes and the surrounding material resulting in slightly higher outlet temperature during heat injection and slightly lower outlet temperatures during heat extraction. In the laboratory TRT, this overestimation of outlet temperature is limited to 0.6 °C (equivalent to underestimating the heat flux by

14 W/m), whereas in the field TRT, the maximum difference between computed and measured outlet temperature is 1.6 °C (equivalent to underestimating the heat flux by 13 W/m).

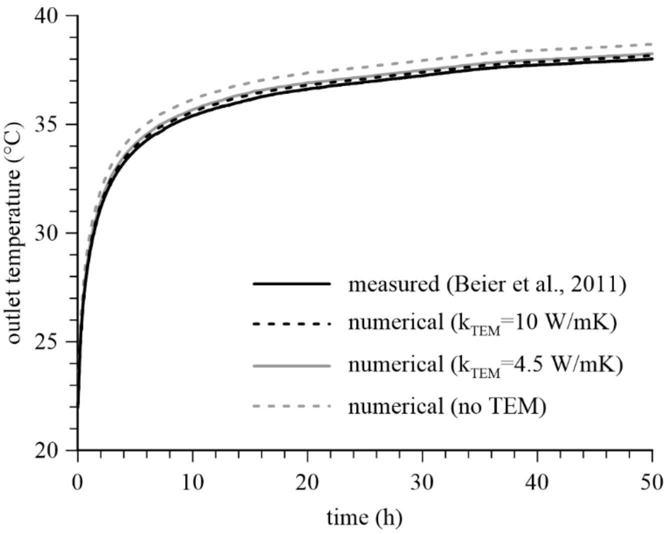

Figure 13 Comparison of outlet fluid temperatures obtained from the laboratory TRT (Beier et al., 2011) and the numerical analyses

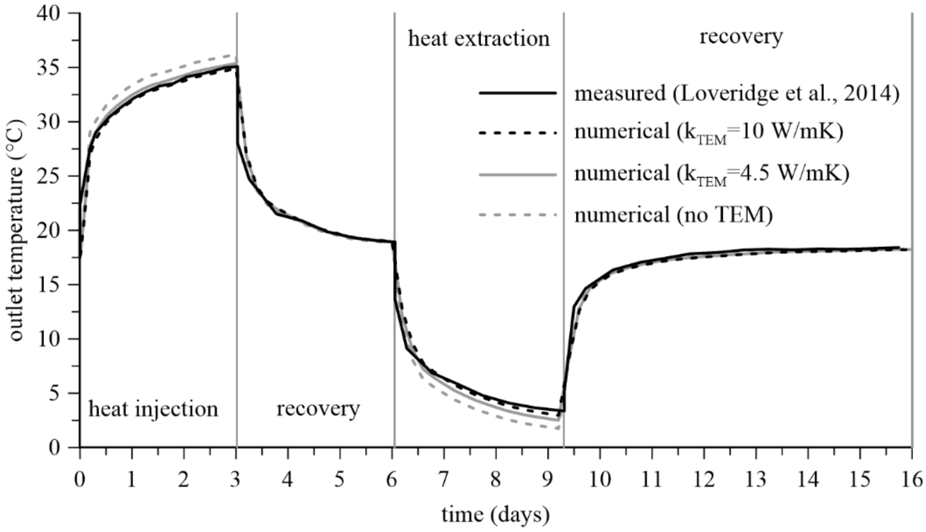

Figure 14 Comparison of outlet fluid temperatures obtained from the field TRT (Loveridge et al., 2014) and the numerical analyses

The effect of the TEM is more pronounced in Figure 15 and Figure 16 which show the temperature evolution in the surrounding medium. It can be seen that the results of the analyses which account for the pipe wall (i.e. k_{TEM} of 4.5 W/mK) result in the best agreement with the measured data, with the maximum difference between the computed and measured temperatures being approximately 0.7 °C and 1.0 °C for the lab TRT and the field TRT, respectively. The analyses with k_{TEM} of 10 W/mK overestimate the heat transfer from the pipe to the surrounding soil, leading to temperature differences limited to 1.1 °C and 2.2 °C for the lab TRT and the field TRT, respectively, whereas the modelling approach which excludes the TEM underestimates the heat transfer, resulting in maximum temperature differences of 2.7 °C and 1.8 °C for the lab TRT and the field TRT, respectively. Therefore, it can be concluded that in order to reproduce the temperature field in the proximity to the heat exchanger pipes, the TEM should be assigned a thermal conductivity which accounts for the effect of the pipe wall.

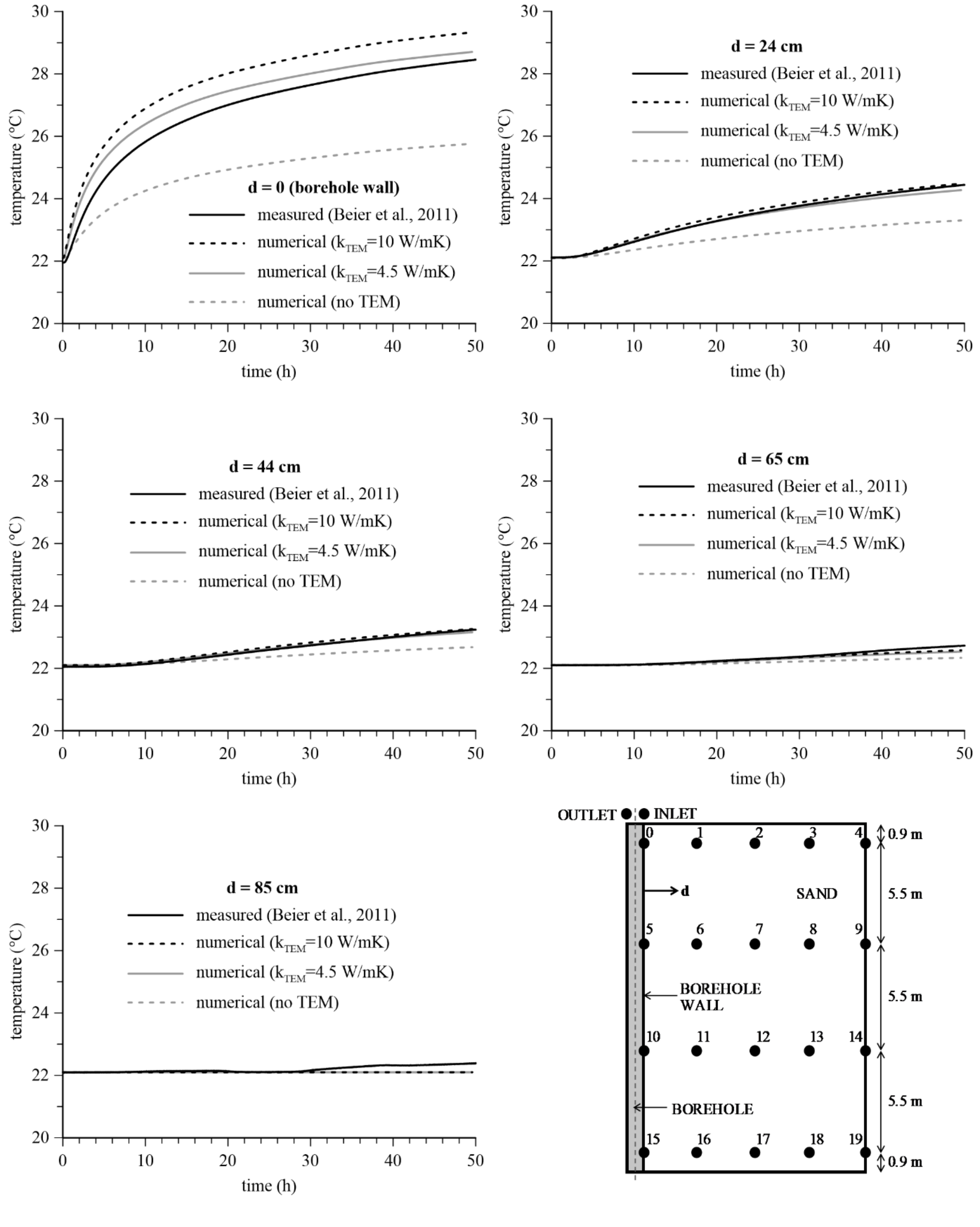

Figure 15 Comparison of measured (Beier et al., 2011) and computed average temperatures at different distances from the borehole in the laboratory TRT

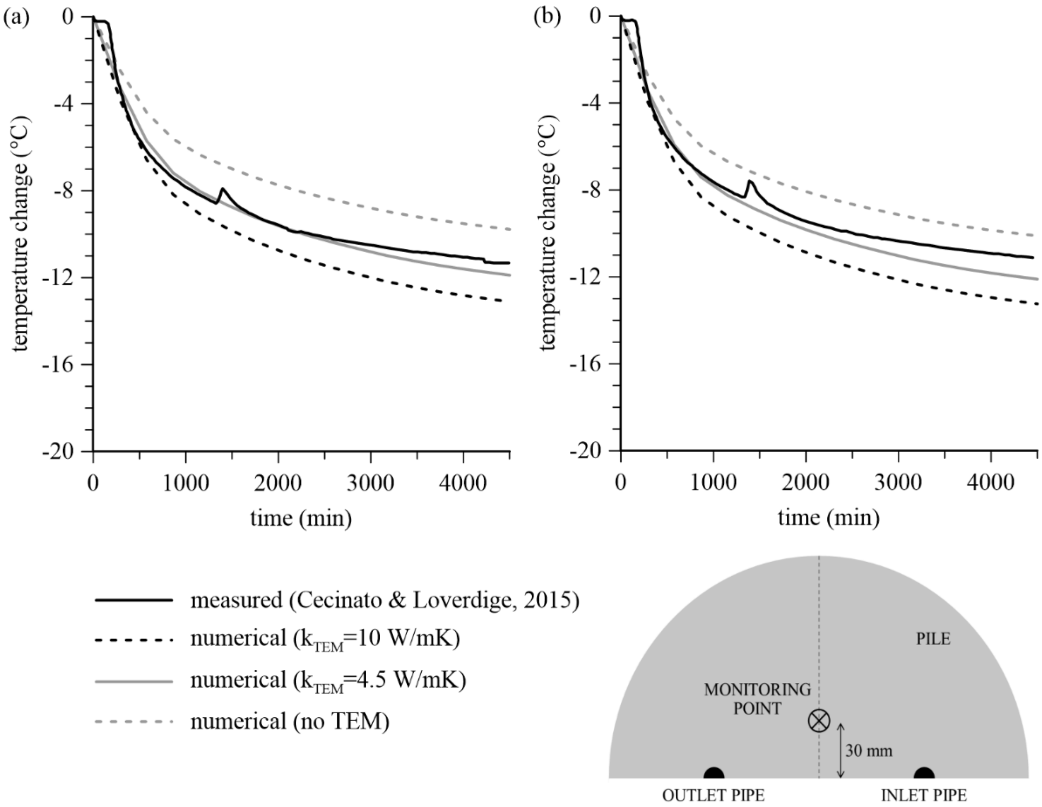

Figure 16 Comparison of measured (Cecinato & Loveridge, 2015) and computed temperature changes in the grout at the depths of (a) 13.8 m, and (b) 23.8 m during the heat extraction stage of the field TRT

Conclusions

This paper presents an alternative robust FE approach for modelling GSES involving heat exchanger pipes whose key features can be summarised as follows:

- The conductive-advective heat flux inside the heat exchanger pipes is simulated using line elements (here referred to as 3D beam elements), whereas solid elements are used for the surrounding materials (e.g. soil, grout). The use of line elements rather than solid elements for modelling the coupled heat and fluid flow along the pipe significantly reduces the number of degrees of freedom in the problem, and hence, the computational effort.
- The conductive-advective heat flux along the pipes is solved using the Petrov-Galerkin FEM instead of the conventional Galerkin FEM which has been shown to produce erroneous solutions characterised by numerical oscillations.

- The heat transfer between the fluid and the surrounding material is simplified by neglecting the effects of heat convection adjacent to the pipe wall.
- Due to the one-dimensional nature of the elements employed as heat exchanger pipes, to account for the effect of the contact area and the interaction mechanisms between the heat exchanger pipe and the surrounding medium a special material with enhanced thermal properties and the same cross-sectional area as the pipe being simulated is placed around the 3D beam elements. This new material is termed the Thermally Enhanced Material (TEM) and is discretised with solid elements.
- As only conductive heat transfer is modelled within the TEM, this approach is more computationally efficient compared to simulating coupled fluid and heat flow inside solid elements representing the inside of the heat exchanger pipe.
- The appropriate thermal conductivity of the TEM was established by performing a comprehensive numerical study and was found to depend on the pipe diameter according to Equation (13) if the effect of the pipe wall is to be accounted for. If the effect of the pipe wall is to be ignored, the thermal conductivity should be 10 W/mK independently of the pipe diameter.

This new modelling approach was validated by reproducing two thermal response tests – one performed on a small scale borehole heat exchanger (Beier et al., 2011) and one performed on a full scale pile (Loveridge et al., 2014). In both cases, the results of the 3D simulations with the TEM are in excellent agreement with the measured data demonstrating the accuracy of the proposed modelling approach. It was shown that in order to simulate the measured heat transfer between the pipe and surrounding ground, the TEM must be included, although the analyses with k_{TEM} of 10 W/mK or one which accounts for the pipe wall produced very similar results. This suggests that either value would be adequate when assessing the thermal performance of a heat exchanger. However, if the temperature field within its cross section or in its immediate vicinity are to be reproduced with a high degree of accuracy, then the performed numerical analyses demonstrate that the effect of the pipe wall needs to be taken into account by using an appropriate value of k_{TEM}. Lastly it should be noted that, when the

TEM is not included and the pipe is modelled with 3D beam elements only, the results appear to be conservative in the short term from the point of view of thermal design, although the effect of the TEM was shown to reduce in the long term.

The success of this validation exercise indicates that the new approach can be used in modelling of more complex problems involving GSES, such as thermally active geotechnical structures. The explicit consideration of variables that affect heat transfer in GSES (e.g. pipe size and configuration, fluid type and flow rate, etc.) is vital for the correct prediction of the thermal performance, and consequently, the structural performance in the case of thermo-active structures. Therefore, the proposed approach enables a more realistic and accurate simulation of GSES than simplified modelling methods where the thermal load is considered by applying a temperature or a flux boundary condition.

Acknowledgements

The research presented in this paper was funded by the Engineering and Physical Sciences Research Council (EPSRC, grant number: 1386304), the Department of Civil and Environmental Engineering, Imperial College London, through a Skempton Scholarship, and the Geotechnical Consulting Group (GCG).

Notation

C_{pf}	fluid specific heat capacity [J/(kg K)]
C_{ps}	solid specific heat capacity [J/(kg K)]
dV	infinitesimal volume [m^3]
D	pipe diameter [m]
h	convective heat transfer coefficient [W/(m^2 K)]
k_T	thermal conductivity [W/(m K)]
k_{TEM}	thermal conductivity of TEM [W/(m K)]
l	pipe length [m]
L	characteristic length [m]

Pe	Péclet number [-]
Q	heat pump power [W]
Q^f	fluid source or sink [m^3]
Q^T	heat source or sink [W]
Q_a	advective heat flux [W]
Q_c	convective heat flux [W]
Q_d	conductive heat flux [W]
Q_f	fluid flow rate [m^3/s]
Q_T	total heat flux [W]
t	time [s]
T	temperature [K]
T_{av}	mean fluid temperature [K]
T_{in}	pipe inlet temperature [K]
T_{out}	pipe outlet temperature [K]
T_r	reference temperature [K]
v_f	fluid velocity [m/s]
ΔT	temperature difference [K]
ρ_f	fluid density [kg/m^3]
ρ_s	solid density [kg/m^3]
Φ_T	heat content per unit volume [J/m^3]

References

Abdelaziz, S. L. A. M. & Ozudogru, T. Y. (2016) Selection of the design temperature change for energy piles. *Applied Thermal Engineering*, 107 1036-1045.

Al-Khoury, R. (2012) *Computational Modeling of Shallow Geothermal Systems.* Multiphysics Modeling. Boca Raton, Taylor & Francis.

Al-Khoury, R. & Bonnier, P. G. (2006) Efficient finite element formulation for geothermal heating systems. Part II: transient. *International Journal for Numerical Methods in Engineering*, 67 (5), 725-45.

Al-Khoury, R., Bonnier, P. G. & Brinkgreve, R. B. J. (2005) Efficient finite element formulation for geothermal heating systems. Part I: Steady state. *International Journal for Numerical Methods in Engineering*, 63 (7), 988-1013.

Banks, D. (2012) *An Introduction to Thermogeology: Ground Source Heating and Cooling.* 2nd Edition. Chichester, Wiley-Blackwell.

Batini, N., Rotta Loria, A. F., Conti, P., Testi, D., Grassi, W. & Laloui, L. (2015) Energy and geotechnical behaviour of energy piles for different design solutions. *Applied Thermal Engineering*, 86 199-213.

Beier, R. A., Smith, M. D. & Spitler, J. D. (2011) Reference data sets for vertical borehole ground heat exchanger models and thermal response test analysis. *Geothermics*, 40 (1), 79-85.

Bidarmaghz, A., Narsilio, G. A., Johnston, I. W. & Colls, S. (2016) The importance of surface air temperature fluctuations on long-term performance of vertical ground heat exchangers. *Geomechanics for Energy and the Environment*, 6 35-44.

Brooks, A. N. & Hughes, T. J. R. (1982) Streamline upwind/Petrov-Galerkin formulations for convection dominated flows with particular emphasis on the incompressible Navier-Stokes equations. *Computer Methods in Applied Mechanics and Engineering*, 32 (1), 199-259.

Caulk, R., Ghazanfari, E. & McCartney, J. S. (2016) Parameterization of a calibrated geothermal energy pile model. *Geomechanics for Energy and the Environment*, 5 1-15.

Cecinato, F. & Loveridge, F. A. (2015) Influences on the thermal efficiency of energy piles. *Energy*, 82 1021-1033.

Çengel, Y. A. & Ghajar, A. J. (2011) *Heat and Mass Transfer: Fundamentals and Applications.* 4th Edition. New York, McGraw-Hill.

Christie, I., Griffiths, D. F., Mitchell, A. R. & Zienkiewicz, O. C. (1976) Finite element methods for second order differential equations with significant first derivatives. *International Journal for Numerical Methods in Engineering*, 10 (6), 1389-1396.

COMSOL (2012a) *COMSOL Multiphysics* [Software] Avaliable from: www.comsol.com.

COMSOL (2012b) *COMSOL Multiphysics Reference Guide (version 4.3a).* COMSOL Multiphysics.

Cui, W., Gawecka, K. A., Potts, D. M., Taborda, D. M. G. & Zdravković, L. (2016) Numerical analysis of coupled thermo-hydraulic problems in geotechnical engineering. *Geomechanics for Energy and the Environment*, 6 22-34.

Cui, W., Gawecka, K. A., Potts, D. M., Taborda, D. M. G. & Zdravkovic, L. (2018a) A Petrov-Galerkin finite element method for 2D transient and steady state highly advective flows in porous media. *Computers and Geotechnics*, 100 158-173.

Cui, W., Potts, D. M., Zdravković, L., Gawecka, K. A. & Taborda, D. M. G. (2018b) An alternative coupled thermo-hydro-mechanical finite element formulation for fully saturated soils. *Computers and Geotechnics*, 94 22-30.

Dassault Systèmes (2017) *Abaqus Unified FEA* [Software] Paris, France. Avaliable from: www.3ds.com/products-services/simulia/products/abaqus.

De Carli, M., Tonon, M., Zarrella, A. & Zecchin, R. (2010) A computational capacity resistance model (CaRM) for vertical ground-coupled heat exchangers. *Renewable Energy*, 35 (7), 1537-50.

Dick, E. (1983) Accurate Petrov-Galerkin methods for transient convective diffusion problems. *International Journal for Numerical Methods in Engineering*, 19 (10), 1425-1433.

Diersch, H. J. G., Bauer, D., Heidemann, W., Ruhaak, W. & Schatzl, P. (2011a) Finite element modeling of borehole heat exchanger systems. Part 1. Fundamentals. *Computers and Geosciences*, 37 (8), 1122-1135.

Diersch, H. J. G., Bauer, D., Heidemann, W., Ruhaak, W. & Schatzl, P. (2011b) Finite element modeling of borehole heat exchanger systems. Part 2. Numerical simulation. *Computers and Geosciences*, 37 (8), 1136-1147.

Donea, J. & Huerta, A. (2003) *Finite Element Methods for Flow Problems.* Chichester, John Wiley & Sons.

Farouki, O. T. (1981) *Thermal Properties of Soils.* Hanover, United States Army Corps of Engineers, Cold Regions Research and Engineering Laboratory.

Gawecka, K. A., Potts, D. M., Cui, W., Taborda, D. M. G. & Zdravković, L. (2018) A coupled thermo-hydro-mechanical finite element formulation of one-dimensional beam elements for three-dimensional analysis. *Computers and Geotechnics*, 104 29-41.

Huyakorn, P. S. (1977) Solution of steady-state, convective transport equation using an upwind finite element scheme. *Applied Mathematical Modelling,* 1 (4), 187-195.

Incropera, F. P., DeWitt, D. P., Bergman, T. L. & Lavine, A. S. (2007) *Fundamentals of Heat and Mass Transfer.* 6th Edition. Hoboken, John Wiley & Sons.

Lazzari, S., Priarone, A. & Zanchini, E. (2010) Long-term performance of BHE (borehole heat exchanger) fields with negligible groundwater movement. *Energy,* 35 (12), 4966-4974.

Loveridge, F., Powrie, W. & Nicholson, D. (2014) Comparison of two different models for pile thermal response test interpretation. *Acta Geotechnica,* 9 (3), 367-384.

Ozudogru, T. Y., Olgun, C. G. & Senol, A. (2014) 3D numerical modeling of vertical geothermal heat exchangers. *Geothermics,* 51 312-324.

Potts, D. M. & Zdravković, L. (1999) *Finite Element Analysis in Geotechnical Engineering: Theory.* London, Thomas Telford.

Ramakrishnan, C. V. (1979) An upwind finite element scheme for the unsteady convective diffusive transport equation. *Applied Mathematical Modelling,* 3 (4), 280-284.

Svec, O. J., Goodrich, L. E. & Palmer, J. H. L. (1983) Heat transfer characteristics of in-ground heat exchangers. *International Journal of Energy Research,* 7 (3), 265-278.

VDI (2010) *VDI 4640 – Blatt 1.* Thermal use of the underground: fundamentals, approvals, environmental aspects. Düsseldorf, Verein Deutscher Ingegneure.

Westerink, J. J. & Shea, D. (1989) Consistent higher degree Petrov–Galerkin methods for the solution of the transient convection–diffusion equation. *International Journal for Numerical Methods in Engineering,* 28 (5), 1077-1101.

Yu, C. C. & Heinrich, J. C. (1986) Petrov-Galerkin methods for the time-dependent convective transport equation. *International Journal for Numerical Methods in Engineering,* 23 (5), 883-901.

Yu, C. C. & Heinrich, J. C. (1987) Petrov-Galerkin method for multidimensional, time-dependent, convective-diffusion equations. *International Journal for Numerical Methods in Engineering,* 24 (11), 2201-2215.

Zanchini, E. & Terlizzese, T. (2008) Finite-Element evaluation of thermal response tests performed on U-tube borehole heat exchangers. In: *Proceedings of the COMSOL Conference, 4-6 November 2008, Hannover, Germany.*

Zienkiewicz, O. C., Taylor, R. L. & Nithiarasu, P. (2014) *The Finite Element Method for Fluid Dynamics.* 7th Edition. Oxford, Elsevier Butterworth-Heinemann.